In nuclear medicine we are more enthused about volume rendering than surface rendering, because our borders are so fuzzy, and (of greater importance) our unique medical information is contained within those borders.

J.M. Links, 1995

Chapter 4

Normal Fusion for 3D Integrated Visualization of SPECT and MR Brain Images

Abstract

Multimodality visualization aims at efficiently presenting integrated information obtained from different modalities, usually combining a functional modality (SPECT, PET, fMRI) with an anatomical modality (CT, MRI). This chapter presents a technique for 3D integrated visualization of SPECT and MR brain images, where MRI is used as a framework of reference for the display of the SPECT data. **Methods:** A novel technique for 3D integrated visualization of functional and anatomical information, called Normal Fusion, is presented. With this technique local functional information is projected onto an anatomic structure. **Results:** The Normal Fusion technique is applied to three cases of SPECT/MRI integration. The results are presented, discussed and evaluated for clinical relevance. **Conclusions:** The results for 3D integrated display of SPECT and MR brain images indicate that the Normal Fusion technique provides a potentially comprehensive and diagnostically valuable presentation of cerebral blood perfusion in relation to the anatomy of the brain.

4.1 Introduction

The use of multiple imaging modalities for clinical examinations is gradually increasing (Maisey et al. 1992, Viergever et al. 1992). The goal of multimodality visualization is to comprehensibly conjoin the diagnostic information of different imaging modalities, and to communicate the integrated information to the referring specialists. The combination of complementary data from multiple modalities may reveal additional diagnostic information as compared with interpretation directly from the individual imaging modalities (Levin et al. 1989, Pelizzari et al. 1989, Holman et al. 1991, Valentino et al. 1991, Hill et al. 1992). We distinguish two types of multimodality integration, *viz.*; *i)* the combination of anatomical data from different modalities, and *ii)* the combination of functional with anatomical data.

An example of the integration of multimodal anatomical information is the fusion of CT and MRI in skull base surgery, where it is used to determine the precise location of a lesion (MRI data) with respect to bone (CT data) in order to obtain a more accurate diagnosis and treatment (Ruff et al. 1993). Other examples of CT/MRI fusion, *e.g.*, for radiation therapy planning, can be found in (Chen and Pelizzari 1989, Van den Elsen and Viergever 1994, Van Herk and Kooy 1994, Van den Elsen et al. 1995, Maintz et al. 1996a); in all these cases the complementarity of the information obtained from CT and MRI is utilized.

Multimodality display can also integrate functional information from, *e.g.*, PET, SPECT, EEG, MEG, MRSI, or fMRI with anatomical information from MRI or CT (Gevins et al. 1990, Schneider et al. 1990, Holman et al. 1991, Evans et al. 1991, Knufman et al. 1992, Viergever et al. 1992). The anatomical modality then provides a frame of reference for spatially correct interpretation of the functional information. Valentino et al. (1991) states: "In brain imaging in particular, the accurate display of functional and anatomic image data is essential in identifying sites of normal and pathophysiologic function in the brain."

This chapter addresses a novel technique for 3D integrated display of SPECT and MR brain images. When using SPECT in isolation, investigation of functional processes and the correlation with anatomical structures is hampered by the low spatial resolution (Mazziotta and Koslow 1987, Kundel 1990, Zubal et al. 1995, Evans et al. 1996). Two options can be applied to facilitate the investigation of SPECT; *i)* the use (and manipulation) of color encoding for the display of SPECT data, so as to employ the potential of the visual system more effectively (Kundel 1990, Stapleton et al. 1994), and *ii)* visually comparing SPECT blood perfusion in pertinent cerebral regions with the homologous regions of the contralateral hemisphere (Kundel 1990, Stapleton et al. 1994, Zubal et al. 1995). To further improve understanding of the underlying relationships between function and anatomy, it is essential that anatomical information, *e.g.*, acquired with CT and/or MRI, is used as a framework for SPECT information (Britton 1994).

Previous studies on simultaneous display of functional and anatomical 2D images

have used linked cursors, alternate pixel display, color integration procedures, and atlasses (Schad et al. 1987, Weiss et al. 1987, Pelizzari et al. 1989, Hawkes et al. 1990). Integrated visualization techniques for SPECT and MR images includes work done by Condon (1991), who implemented five techniques that used SPECT information as an extra dimension (either as height, color or time) to a 2D MR image.

Techniques for 3D multimodality visualization of functional and anatomical data have been used mainly for PET/MRI using windows (Levin et al. 1989), opacity weighted display (Evans et al. 1996), cutplanes (Evans et al. 1991) or mapping functional activity onto the brain surface (Levin et al. 1989, Hu et al. 1990, Valentino et al. 1991). The 3D presentation of SPECT information combined with anatomical information has been primarily focused on the visualization of already detected abnormalities, so that standard volume visualization techniques can be applied (Wallis 1992).

The present study discusses a novel technique, called Normal Fusion, to simultaneously display functional and anatomical data. The—preliminary—evaluation of the method focuses on three cases that investigate the relation between behavioral disorders and functional/morphological brain damage. The cases are: 1) a patient with a frontal lobe tumor (Hulshoff Pol et al. 1995), 2) a patient with autistic behavior, and 3) a patient with the Gilles de la Tourette syndrome (TS). The objectives of our work are to investigate whether *i)* the multimodal information can be presented simultaneously and comprehensively, and *ii)* additional information can be obtained from simultaneous presentation of the data.

The organization of the chapter is as follows: This introduction on multimodality visualization of SPECT and MRI is followed by a brief overview of the acquisition characteristics and the tools that were used. An explanation of the employed volume visualization method precedes a description of the principles and individual merits of the Normal Fusion technique. The visualization results for the three cases are presented and evaluated, followed by the conclusions.

4.2 Acquisition

Information on brain anatomy was acquired from a T1-weighted 3D gradient-echo MR image. The MRI data of the whole head consisted of contiguous axial slices (128 for case 1, 131 for case 2, and 127 for case 3) of 1.3 mm thickness with TR=30 ms, TE=13 ms, 256×256 matrix, and 230 mm FOV. The MR images were acquired with a whole-body Philips Gyroscan 0.5 Tesla using a standard head coil. Information on functional processes in the brain was obtained from a HMPAO–SPECT scan, which portrays the cerebral blood perfusion (Perani et al. 1988). The SPECT data was reconstructed to contiguous axial slices (36 for case 1, 46 for case 2, and 44 for case 3) with a 64×64 matrix, a slice thickness of approximately 7.1 mm, a plane resolution of 7.5 mm FWHM, acquired with a Picker PRISM^{TM} three-detector gamma camera

using a long-bore ultra high resolution, low energy fanbeam collimator.

4.3 Processing and visualization

Registration of the datasets was done using external arrow-shaped skin markers and in-house developed software (Van den Elsen 1993). We chose to match to the MRI data to avoid degradation of the cortex renderings. We used ANALYZE^{TM} (Robb 1990) for the segmentation of the datasets. For the multimodality 3D visualization, we used the software package VROOM (Zuiderveld 1995), developed at our department; it is essentially a collection of C++ classes aimed at multimodality visualization.

4.4 3D integrated visualization

Realistic images of 3D medical volume data on a computer monitor can be obtained with a process called volume visualization. The demand for volume visualization of 3D imaging data in routine clinical work is rapidly increasing. This is true not only for the analysis of the data by the radiologist or the nuclear medicine physician, but also, and maybe more importantly, for communication with the referring physician or surgeon. For example, brain surface structures are generally hard to identify for lack of anatomical information when using 2D images only. With the help of a 3D rendering of the brain, gyri and sulci are much easier to trace, which alleviates the study of brain anatomy (Kundel 1990, Höhne and Hanson 1992, Kikinis et al. 1992).

4.4.1 Visualization of anatomical surfaces

Volume visualization relies on shading techniques to model the light absorption, reflection, and transmission along surfaces. In general, photorealism is not required, which is why simple techniques can be used to achieve adequate visualization speeds.

The first assumption is a single light source at an infinite distance, while shadowing is usually ignored. This implies that the light intensity as well as its direction is constant across the entire volume to be visualized.

A further simplification of the process is the use of orthographic instead of perspective projection. This considerably simplifies and speeds up the visualization process, which is why orthographic projection is still often used.

In general, modern 3D visualization techniques calculate the surface direction from the original grey data. The surface normal can be represented by the normalized grey level gradient (Höhne et al. 1990). For every point on a surface this gradient can be calculated from the grey level data of its neighbors (*e.g.*, six first order neighbors or in a second order ($3\times3\times3$) neighborhood). Normalization of the gradient subsequently yields the (outward) surface normal.

A simple light reflection model suffices in most cases. The most used light model is that of Phong (Phong 1975), which separates the reflected light into three components, *viz.*; *i)* an ambient, *ii)* a diffuse, and *iii)* a specular component. Furthermore, a significant reduction in visualization speed can be obtained by approximation of the specular component (Schlick 1994).

The demand for 3D volume visualization is even more stringent for multimodal datasets, where mental 3D reconstruction of the multivariate information is nigh impossible. In this chapter, we present a novel technique for 3D integrated visualization of SPECT and MRI. The technique Normal Fusion color encodes local SPECT activity onto the brain surface rendered from MRI.

4.4.2 Normal Fusion

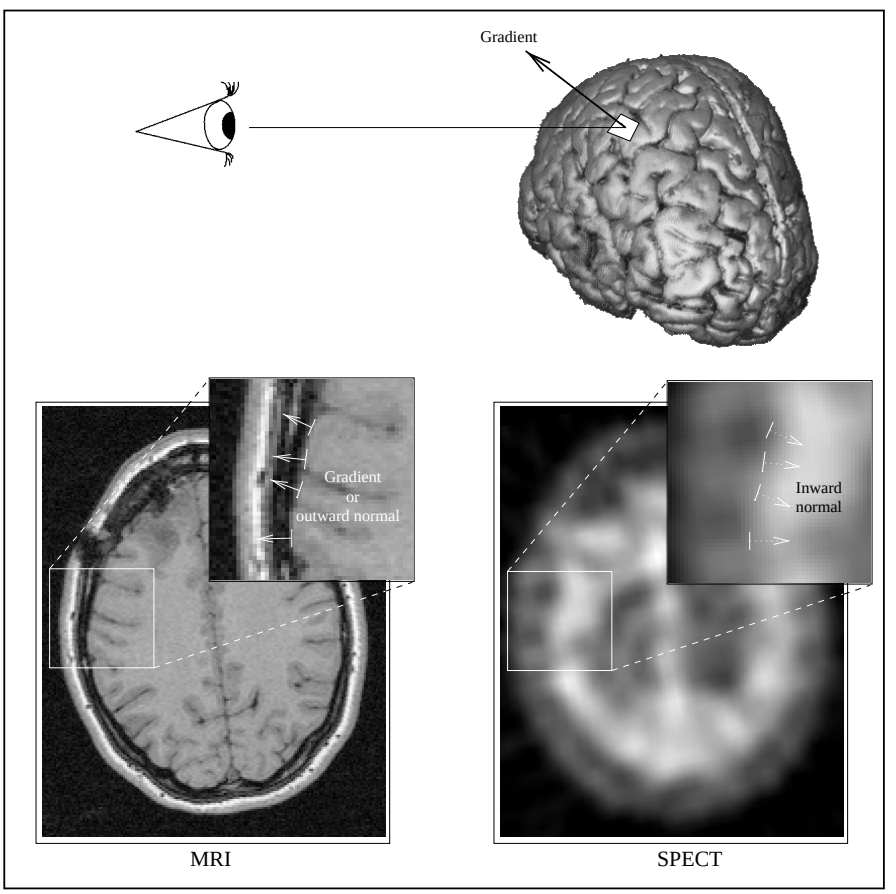

Figure 4.1 *Principle of the Normal Fusion technique. The gradient calculated in a standard volumetric rendering procedure of MR images is used to evaluate the corresponding SPECT data.*

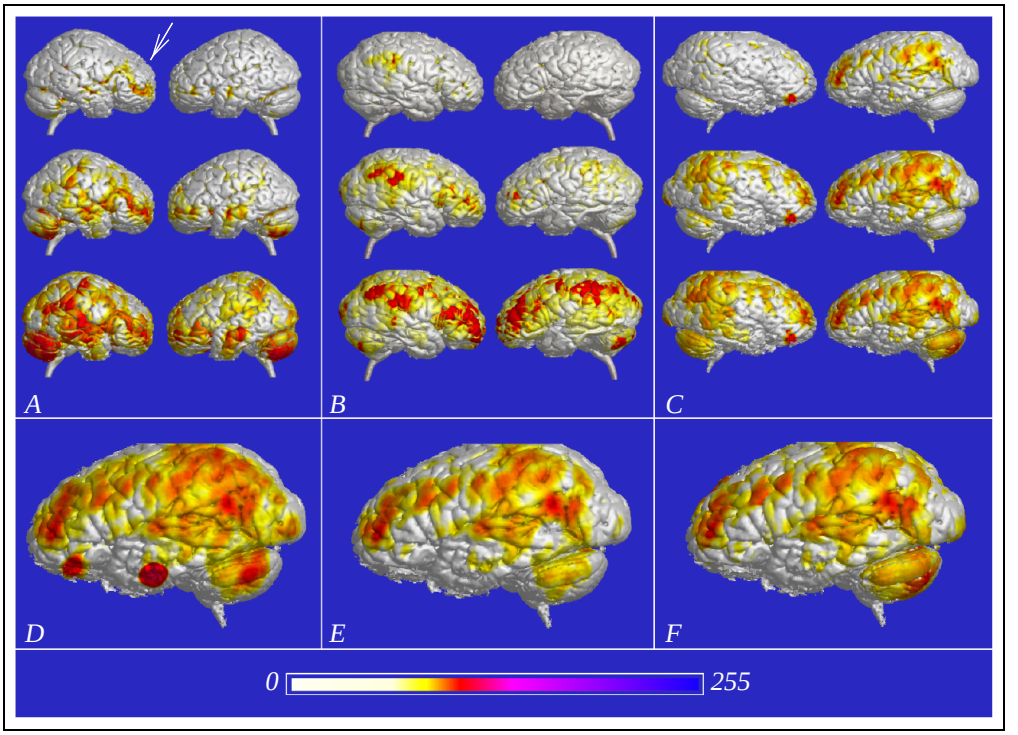

Figure 4.2 *See page 65.*

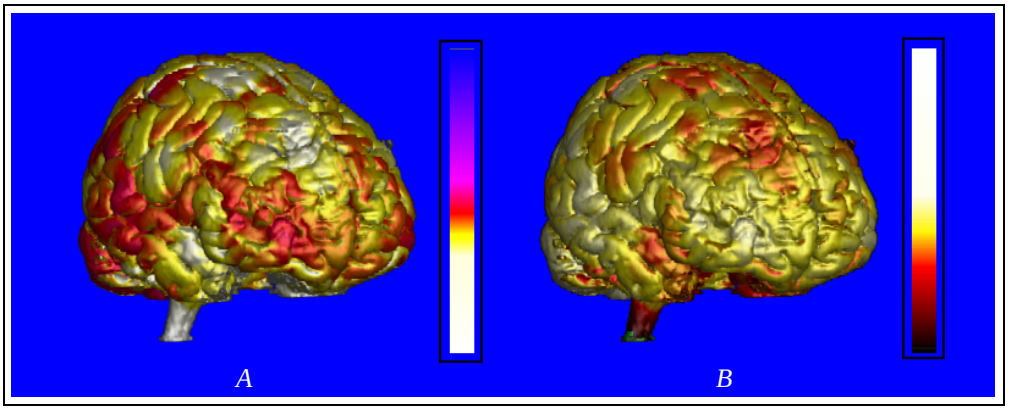

Figure 4.3 *Normal Fusion visualization using the maximum value of the SPECT samples to color encode the surface. Frame (A): Color encoding with the lookup table proposed in the present chapter. Frame (B): Color encoding with the original heated-object scale.*

← **Figure 4.2** *Top part: Surface color encoding of SPECT activity on a brain surface for a patient with a right frontal lobe tumor (see arrow) (A), a patient with autistic behavior (B), and a patient with TS (C). For these three cases 3D renderings of the right and left hemisphere with different depth ranges are presented; 0–1 mm (top row), 0–5 mm (middle row), and 0–10 mm (bottom row). The maximum value over the depth range was used to color encode the corresponding surface voxel. Bottom part: Influence of the integration direction on the multimodality visualization. The renderings in Frames (D) and (E) are the result of fusion employing the viewing direction. Both images color encode the highest activity onto the surface, Frame (D) traverses the whole dataset, Frame (E) uses only the first 10 mm. Frame (F) results from the Normal Fusion technique depicting the highest activity over a depth of 10 mm. The portrayed lookup table was the basis for the color encoding; scaling was adjusted for each case accordingly.*

HMPAO–SPECT images portray the cerebral blood perfusion (Roper et al. 1991, Matsuda et al. 1993, Faber and Folks 1994), which is tightly coupled with the activity of the tissue. Activity in the brain is mainly located in the grey matter (Valentino et al. 1991), whose principal part is the folded surface layer (about 2–10 mm thick). Various methods that map functional activity of the grey matter onto the brain surface rendered from anatomical data have already been proposed (Levin et al. 1989, Hu et al. 1990). These techniques share the characteristic that the functional activity below the surface is sampled along the viewing direction. From these samples a value is calculated which is color encoded onto the surface. The resulting visualizations provide the observer with specific information concerning brain function in relation to anatomy. However, the obtained functional information is a representation of information integrated along the viewing direction rather than the actual local activity beneath the brain surface. We developed a technique to investigate the functional activity more accurately making use of the gradient that is calculated in the volume visualization process.

Normal Fusion spawns a secondary ray at the surface along the reverse gradient or inward normal direction (see Figure 4.1). With SPECT/MRI visualization, we use this secondary ray to project local functional brain activity from SPECT onto the surface rendered from MRI–T1 data. The value at a surface voxel is calculated from sample points of SPECT in the direction of the inward normal; integration depth and sampling rate are user definable. The surface voxel has been calculated in two ways (other methods can be implemented easily), *viz.*; *i)* by taking the average of the sample values, and *ii)* by taking the maximum intensity value along the sample direction (MIP). The obtained value represents the cerebral blood perfusion just below the surface. The calculated activity is then color encoded onto the volumetric rendering of the cortex as derived from the MRI data.

The integrated display shown in Figure 4.2 (Frames *A*, *B*, and *C*) is the result of

the Normal Fusion procedure applied to the SPECT/MRI datasets of the three cases using different depths (top row for a depth of 1 mm, middle row for 5 mm, and the bottom row for 10 mm), one sample per mm, and color encoding the maximum SPECT value onto the surface of the brain.

The results of the patient with the frontal lobe tumor (case 1) are presented in Figure 4.2*A*. The left hemisphere (right column) portrays SPECT activity (cerebral blood perfusion) beneath the surface of an assumed healthy brain hemisphere. The right hemisphere (left column) shows how the deterioration of gyri and sulci, as is visible from the MRI cortex data (see arrow), matches the abnormal region visible from the color encoded SPECT activity. The abnormal gyral pattern is hypoperfused in accordance with the presence of a tumor underneath this surface region. We observe that a strip of increased activity, corresponding with increased blood perfusion beneath the surface, surrounds the damaged region. Furthermore, the right hemisphere and cerebellum show an overall increase in activity compared to the left hemisphere and cerebellum, apparently no diaschysis is present.

The results of case 2, a patient with autistic behavior are shown in Figure 4.2*B*. It shows several differences between left and right hemisphere, *viz.*; *i)* frontal lobe hyperperfusion, left hemisphere slightly higher than the right, and *ii)* left temporal hypoperfusion. Although the gyration appeared normal on the 2D MR images, the 3D volume rendering is suggestive of an abnormal gyral pattern of the left temporal lobe. Noteworthy is an absence of perfusion in the area of Wernicke.

The results of case 3, a TS patient, are presented in Figure 4.2*C*. The top of the brain was not scanned. Several differences between left and right hemisphere can be noted, *viz.*; *i)* a strong hot-spot in the right lateral fronto-orbital region which is already clearly visible at a depth of 1 mm, *ii)* increased activity in the left dorsal parietal lobe over a diffuse area, and *iii)* increased activity in the left dorsal cerebellum, with a normal right cerebellum.

The findings of all three cases were based on both the 2D SPECT data and the 3D Normal Fusion images. Some of the reported findings were difficult to establish upon examining the 2D SPECT slices only. Moreover mental reconstruction of the 3D activity in relation to the anatomy appeared a difficult task.

Standard SPECT lookup tables were not suitable for our applications, because their low-activity colors are shades of black. An instructive simultaneous presentation of the cortical hot-spots in SPECT in relation to the MRI data was obtained upon adjusting the heated-object scale such that the low-activity color was changed from black to blue and the scale was reverted (see Figure 4.3). While this lookup table is valid for these three cases, visualization of other cases (*e.g.*, for visualization of cold-spots) may require a different lookup table. The option to (rapidly) change the color encoding of the calculated surface value by manipulation of the lookup table appears a valuable extension of this visualization technique.

We have studied the effect of different depths and sampling rates on the final visualization, as well as different strategies for deriving a surface value from the

activity beneath the surface. With the sampling rate, a trade-off between accuracy and speed exists. The sampling rate should be high enough to accurately sample the SPECT data, but preferably as low as possible for a quick assessment of the visualization result. The evaluation strategy depends on the information the observer is interested in. For instance, MIP appears to be the method of choice to reveal hot-spots, but the averaging method may be more suitable to give an impression of the entire range of sampled SPECT intensities. Other data and applications may demand different calculation paradigms. Changing the depth, or better, the depth range, over which the SPECT data are sampled offers the possibility to reveal superficial or more deeper lying regions of activity. With case 3, the hot-spot in the right lateral fronto–orbital region could already be appreciated using only the first voxel of SPECT information below the brain surface. Other hot-spots did not emerge until the depth was increased to 10 mm (see Figure 4.2*C*) or beyond.

One of the main advantages of the Normal Fusion method is that it follows the curvature of the brain to calculate the regional activity of subcortical cells, which makes the visualization independent of the viewing direction. Earlier techniques (*e.g.*, for PET/MRI see (Levin et al. 1989, Hu et al. 1990)) made use of the viewing direction to integrate information onto the surface of the brain. To illustrate the effect of the integration direction, we rendered the left hemisphere of case 3 with three methods. The first method used the viewing direction through the entire volume (see Figure 4.2*D*), the second used the viewing direction with a depth of 10 mm (see Figure 4.2*E*), and the third used the inward normal direction with a depth of 10 mm (see Figure 4.2*F*). For all three methods we used one sample per mm, while the maximum value was calculated to color encode the surface.

In Figure 4.2*D* two clearly delineated hot-spots are visible in the left inferior frontal and left inferior temporal region. The first hot-spot stems from the right lateral fronto-orbital region (see Figure 4.2*C*) and the second hot-spot is activity from the fiducial marker attached to the right temporo-mandibular skin surface. In the parietal and occipital region there are other hot-spots that result from right hemisphere activity. The effect of activity in the right hemispere visible on the left hemisphere is greatly reduced when the depth is decreased as can be seen in Figure 4.2*E*. Still, activity depicted on the surface of a gyrus may result from activity located in a neigboring gyrus. This effect can best be appreciated in a movie-sequence where the angle-of-view is changed. Then the location, form, and color of the hot-spots changes for each angle. The activity of the cerebellum, which can be used as a reference (Hashikawa et al. 1995), also changes with the viewing angle. The dependency on the angle-of-view proved large (*esp.* when using the entire volume), which reduces the ability to correctly localize activity. Figure 4.2*F* depicts the rendering with the Normal Fusion technique, which is insensitive to the viewing direction. From each viewing angle the colors on the surface remain exactly identical.

An extensive clinical evaluation of multimodality visualization techniques is in progress (see Chapter 6). This will require many more datasets that are currently

collected. Below, we give a first impression of the validity of the Normal Fusion approach based upon the three cases shown in this section.

4.5 Assessment of clinical relevance

A preliminary evaluation of the Normal Fusion technique was carried out by five nuclear medicine physicians of the University Hospital Utrecht. They answered a set of simple, yet fundamental questions so as to assess the possible clinical benefits of the technique. Since we report on three cases only and anticipated a training effect, we decided to conduct the evaluation twice for each observer with at least one week between the two sessions.

The cases were presented to each of the nuclear medicine physicians separately and consisted of the usual SPECT data in the familiar setting of their own department. The order was identical for each nuclear medicine physician, *viz.* case 1, case 2, and then case 3. First, the physician was asked to perform a routine clinical screening of the patient data with the original clinical information at hand. For case 1 this information was: Operation because of a histologically confirmed right frontal asterocytome grade II (see also the 2D image data in Figure 4.1). Question: How is the surrounding cerebral bloodflow? For case 2: Dysfunction related to autism. Question: Abnormalities frontal region and basal ganglia? For case 3: Tourette syndrome. Question: Perfusion abnormalities in basal ganglia?

Subsequently, preprocessed Normal Fusion images were added depicting the highest SPECT activity on the brain surface for four depths (1, 5, 10, and 15 mm.) and for four viewing angles (from the frontal, right, left, and caudal side of the brain). The right and left views over depths of 1, 5, and 10 mm for the three cases are depicted in Figures 4.2*A*, *B*, and *C*. The following list of questions had to be answered for the presentation of each case:

1. Do you find it difficult to relate the information acquired from the Normal Fusion technique to the traditional 2D SPECT images for this case?
2. Is the Normal Fusion technique beneficial in establishing an anatomical framework for the functional SPECT information for this case?
3. Do you find this framework useful for the investigation of SPECT for this case?
4. Do you expect that this type of presentation will facilitate establishing the differential diagnosis for this case?
5. Do you expect that communication to the referring clinician will be improved with this type of presentation for this case?
6. Do you expect to use the Normal Fusion pictures for a general impression (an overview) when interpreting the 2D SPECT images for this case?

The questions could be answered with: 1=definitely yes, 2=probably yes, 3=neutral, 4=probably no, and 5=definitely no.

	Session 1						Session 2					
	Tumor		Autist		Tourette		Tumor		Autist		Tourette	
Question	mean	s.d.	mean	s.d.	mean	s.d.	mean	s.d.	mean	s.d.	mean	s.d.
Difficult to relate NF to 2D?	3.6	2.0	4.2	0.8	5.0	-	5.0	-	5.0	-	5.0	-
Establishes anatomical framework?	1.2	0.4	2.4	2.0	1.2	0.4	1.0	-	2.2	1.6	1.0	-
Is framework useful?	2.4	1.1	3.4	1.5	1.8	1.8	1.0	-	2.4	1.5	1.6	0.9
Facilitates differential diagnosis?	2.4	0.9	3.4	1.3	3.0	1.9	1.4	0.5	2.4	1.7	1.8	0.4
Communication improved?	1.0	-	3.4	1.8	2.4	1.5	1.0	-	2.6	1.8	1.2	0.4
Use as overview?	1.2	0.4	2.4	1.7	2.6	1.5	1.0	-	2.4	1.5	1.2	0.4

Table 4.1 *Results (two sessions) of the clinical evaluation for three cases: Case 1 is a patient with a right frontal lobe tumor, case 2 is a patient with autistic behavior, and case 3 is a TS patient. A full-length version of the questions can be found in the text and the answers could be either 1=definitely yes, 2=probably yes, 3=neutral, 4=probably no, or 5=definitely no. An arithmetic mean (mean) with standard deviation (s.d.) over all observers was calculated. In all questions but the first, the response "1" is considered positive for the Normal Fusion (NF) technique; in the first question the response "5" is considered positive.*

Although the data are categorical, we decided to calculate an arithmetic mean with standard deviation for computational ease and to facilitate comprehension. The nuclear medicine physicians were not trained to interpret the Normal Fusion images in clinical practice. At first it proved difficult to fully understand and categorize the information conveyed by the Normal Fusion images. After some training, the information from the Normal Fusion images was easily interpreted and integrated with the information from the 2D SPECT images. Especially for cases 1 and 3 (see Table 1), consistency accross the nuclear medicine physicians increased considerably from session 1 to 2 while this was also true for four out of five observers for case 2. The less favorable results for the autistic patient were caused by the deviating opinion of one observer, who attested that the Normal Fusion image for this case conveyed clinically irrelevant or incorrect information.

Initially, the nuclear medicine physicians stated they would use the Normal Fusion images only when the clinical question called for investigation of cortical activity. After the training phase they reported they would use the technique to quickly investigate cortical activity even if the clinical question did not point to the cortex as the primary site of interest. Several of the observers reported a desire to manipulate the color encoding scale of the Normal Fusion images for an improved understanding of the data.

The clinicians appreciated direct (3D) visual comparison with the homologous region of the other hemisphere, especially when the 2D SPECT images were not

properly aligned. Then, investigation of the 2D SPECT images proved problematic, because comparison of activity with the mirror hemisphere was difficult. The Normal Fusion technique is not affected by misalignment of the original 2D SPECT images, because of the provided anatomical framework, which alleviates the comparison with the pertinent anatomical region.

Overall, the results of session 2 (see Table 1) indicate that the observers considered transfer of information from the Normal Fusion images to the 2D SPECT data easy. The technique provides an anatomical framework which may help not only in establishing the differential diagnosis, but also in communicating to the referring clinician.

4.6 Conclusions

There is a growing need for multimodality visualization tools in the clinic to gain more insight into the intricate information conveyed by multimodal datasets. Use of 3D multimodality visualization techniques for SPECT and MRI may facilitate diagnosis and communication by increasing the appreciation of the spatial relationships of the images.

We developed a novel method for the integrated 3D visualization of information acquired with SPECT and MRI. This method, Normal Fusion, calculates the regional blood perfusion beneath the surface and color encodes this value onto the MRI cortex rendering. Functional information of the surface layer of cortical grey matter is presented within an anatomical frame of reference. The curvature of the brain is followed, which makes the visualization independent of the viewing direction.

Experience with this technique using clinical datasets is promising. Information that was difficult to find when diagnosing SPECT from the individual slices was brought out by the multimodal presentations. A simple clinical evaluation of the Normal Fusion technique was conducted, which indicated that communication and anatomical localization may well benefit from this technique. The promising evaluation results call for a rigorous validation of the diagnostic value of the Normal Fusion technique, or rather more generally of simultaneous display of functional and anatomical information.

Acknowledgements

We are indebted to our colleagues P.C. Anema, P.C. van Barneveld, F.J. Beekman, J. Buitelaar, W.I. de Bruin, E. Buskens, P.A. van den Elsen, J.H. de Groot, J.W. van Isselt, R.T.M. Jonk, J.M.H. de Klerk, J.B.A. Maintz, L.C. Meiners, M. Metselaar, and G.R. Timmens for their contributions. We gratefully acknowledge the research licence of ANALYZE^{TM}, provided by Dr R.A. Robb, Mayo Foundation/ Clinic, Rochester, Minnesota.